ESC HEART FAILURE
ESC Heart Failure 2023; **10**: 2479–2486
Published online 5 June 2023 in Wiley Online Library (wileyonlinelibrary.com) **DOI:** 10.1002/ehf2.14417

ORIGINAL ARTICLE

Identification of a novel splicing-altering *LAMP2* variant in a Chinese family with Danon disease

Di Fu, Shuai Wang, Yonghong Luo, Sha Wu and Daoquan Peng*

Department of Cardiovascular Medicine, The Second Xiangya Hospital, Central South University, 410011HunanChangsha, No. 139 Middle Renmin RoadChina

Abstract

Aims This study aimed to identify a novel splicing-altering *LAMP2* variant associated with Danon disease.

Methods and results To identify the potential genetic mutation in a Chinese pedigree, whole-exome sequencing was conducted in the proband, and Sanger sequencing was performed on the proband's parents. To verify the impact of the splice-site variant, a minigene splicing assay was applied. The AlphaFold2 analysis was used to analyse the mutant protein structure. A splice-site variant (NM_013995.2:c.864+5G>A) located at intron 6 of the *LAMP2* gene was identified as a potential pathogenic variant. The minigene splicing revealed that this variant causes exon 6 to be skipped, resulting in a truncated protein. The AlphaFold2 analysis showed that the mutation caused a protein twist direction change, leading to conformational abnormality.

Conclusions A novel splice-site variant (NM_013995.2:c.864+5G>A) located at intron 6 of the *LAMP2* gene was identified. This discovery may enlarge the *LAMP2* variant spectrum, promote accurate genetic counselling, and contribute to the diagnosis of Danon disease.

Keywords Danon disease; *LAMP2*; Splicing mutation; Genetic diagnosis; Minigene assay

Received: 27 December 2022; Revised: 18 April 2023; Accepted: 11 May 2023
**Correspondence to: Daoquan Peng, Department of Cardiovascular Medicine, The Second Xiangya Hospital, Central South University, No. 139 Middle Renmin Road, Changsha, Hunan 410011, China. Tel: +86-731-85292165; Fax: +86-731-85533525. Email: pengdq@csu.edu.cn*

Introduction

Danon disease is an X-linked lysosome-associated membrane protein gene (LAMP2) disease.[1–3] The primary clinical manifestations of this disease are hypertrophic cardiomyopathy, skeletal myopathy, and intellectual disability, which tend to be less severe in females.[4,5] Danon disease is most commonly observed among young males, typically under the age of 20, and often results in mortality prior to age 30.[4,6]

The *LAMP2* gene is situated on the human X chromosome (Xq24) and contains 10 exons.[7,8] The *LAMP2* gene encodes the LAMP2 protein, which consists of 410 amino acids. The LAMP2 protein is a type 1 membrane protein that predominantly locates in the lysosomal compartment. Its structure includes a heavily glycosylated large luminal domain, a transmembrane region, and a short carboxy-terminal cytoplasmic tail.[9] Mutation in the *LAMP2* gene mutation leads to the deficiency of all three *LAMP-2* isoforms (*LAMP-2a*, *LAMP-2b*, and *LAMP-2c*), with isoform-specific mutations being found only in *LAMP-2b*.[2] *LAMP-2b* deficiency results in lysosomal storage disorder and glycogen accumulation in lysosomes, leading to multiorgan damage, especially in the heart and skeletal muscle.[10]

The diagnosis of Danon disease depends on genetic diagnosis, but not all pathogenic genes of Danon disease have been fully screened.[11] In this article, we identified a case of Danon disease characterized by hypertrophic cardiomyopathy with ventricular pre-excitation. The gene analysis revealed a mutation of intron 6 (c.864+5G>A), resulting in splicing over exon 6 (123 bp) and a truncated protein by 41 amino acids. The AlphaFold2 analysis of *LAMP2* predicts that the mutant causes protein twists direction change, leading to its conformational abnormality. This discovery contributes to the expansion of the *LAMP2* variant spectrum of Danon disease.

Methods

The peripheral blood samples of the proband and his relatives were immediately sent for examination following the draw. From these samples, DNA will be extracted using a

Qiagen DNA Blood Midi/Mini kit (Qiagen GmbH, Hilden, Germany). The resulting genomic DNA was processed and integrated into the experimental system (Integrated DNA Technologies, San Diego, USA) to create a sequencing library. Library sequencing was performed on the Agilent Bioanalyzer 2100 (Agilent Technologies, Santa Clara, CA, USA). The data obtained were analysed using the mutation site detection system NovaSeq 6000 platform (Illumina, San Diego, USA) and the variation site annotation interpretation system (enliven, Berry Genomics, Beijing, China).

Sanger sequencing

The identified pathogenic mutations and low coverage regions identified in this study were confirmed by Sanger sequencing, utilizing the forward primer TTGGTAGAGTGTAA GGCTTTGCT and the reverse primer TGAGGGATGAACAGGG ATGAAT on a sequencer. Once validated in the patient, the potential pathogenic mutations were also examined in his parents by Sanger sequencing. This methodological approach ensured the accurate identification and confirmation of the pathogenic mutations and provided valuable information for further study.

Single nucleotide variations analysis

The analysis of single nucleotide variations (SNVs) was conducted using the SNV workflow (Verita Trekker, Berry Genomics) on the targeted sequencing data. To validate any of the potential pathogenic SNVs, we utilized quantitative real-time PCR analysis of gDNA.

Minigene assays

A pair of minigene plasmids (wild type and mutant) was designed for the *LAMP2* gene mutation (NM_013995.2:c.864 +5G>A). The minigene regions spanning *LAMP2* exon 6 with partial intron 5–7 were amplified from the wild-type and mutant gDNA, using the following specific primer pair: wild-type forward primer (5′-AAGCTTGGTACCGAGCTCGGATCCAGTTCCT GTGTGATAAAGACAAAACTTC-3′) with the restriction site BamHI and wild-type primer reverse (5′-ATAATTTCAGTAGT TGCTTCTGAGAAGGTGGAAATAAAG-3′) with the restriction site Xhol, and mutant primer forward (5′-GAAGCAACTACT GAAATTATTAGAATGACTGGCTGATCA-3′) with the restriction site BamHI and mutant reverse primer (5′-TTAAACGGGCCCT TAGACTCGCGGAGCCATTAACCAAATACATGCTGAT-3′) with the restriction site Xhol. By using ClonExpress II One Step Cloning Kit (Vazyme, Nanjing, China), the amplified products were cloned into the pMini-CopGFP vector (Beijing Hitrobio Biotechnology Co., Ltd.).

The human embryonic kidney (HEK-293) cell lines were cultured in Dulbecco's modified Eagle's medium (Thermo Fisher, CA, USA) supplemented with 10% foetal bovine serum from PAN-biotech Germany. The cells were cultured at 37°C with 5% carbon dioxide (CO_2) in a humidified incubator. To perform the cell transfection, Lipofectamine™ 2000 Transfection Reagent (Thermo Fisher) was utilized, following the protocol of the manufacturer.

RNA extraction, cDNA synthesis, and splice-site analysis

HEK-293 cells were transfected in triplicate, and the total RNA was extracted with TRIzol reagent (CoWin Biotech, China) 48 h later. Reverse transcription polymerase chain reaction (RT-PCR) was performed with a pair of primers: MiniRT-F (5′-GGCTAACTAGAGAACCCACTGCTTA-3′) and MiniRT-R (5′-CGGAGCCATTAACCAAATACATGC-3′). The resulting PCR products were visualized through electrophoresis on a 2% agarose gel and confirmed by Sanger sequencing (Tsingke Biotechnology Co., Ltd.).

Protein structural modelling

To investigate the consequence of the identified mutation, the protein structural modelling source code for the AlphaFold2 model, trained weights, and inference script were available under an open-source licence using the AlphaFold2 protein structure database and figures were prepared with PyMOL.

Results

Clinical phenotypes

A 14-year-old adolescent was hospitalized due to the sudden onset of palpitations that occurred 20 days prior to admission. The patient experienced paroxysmal palpitations and brief discomfort at rest, which rapidly subsided. After exercise, the patient experienced several breathing difficulties that resolved after several minutes of rest. The patient did not experience accompanying symptoms, such as chest tightness, chest pain, headache, dizziness, or syncope. The patient demonstrated normal cognitive and physical development and exhibited normal bilateral muscle strength during the physical examination. Additionally, the patient's family history of coronary heart disease was limited to the patient's grandfather.

Laboratory examinations indicated elevated levels of cardiac troponin T (cTnT; 100 pg/mL, normal <14 pg/mL), creatine kinase (CK; 702.6 U/L, normal 50.0–310.0 U/L), and CK-MB (33.8 ng/mL, normal <25 ng/mL). In addition, liver enzymes, such as aspartate aminotransferase (276.2 U/L, nor-

mal 15–40 U/L) and alanine aminotransferase (ALT; 211.6 U/L, normal 9–50 U/L), were increased. The electrocardiogram (ECG) of the patient under observation was found to be significant for a short PR interval (<120 ms) and an extended QRS wave duration (176 ms). Notably, the QRS complex displays a downward main wave in lead V1 and an upward main wave in leads V5 and V6. A comprehensive evaluation of the ECG revealed a pattern of B-type pre-excitation syndrome. Additionally, the ECG also revealed the presence of premature atrial contraction and left ventricular hypertrophy (*Figure 1A*). The patient was followed up during 2021–23, and ECGs are provided in the Supporting Information, *Figure S1*.

On 28th January 2021, colour Doppler echocardiography was performed, which revealed the following measurements: right atrium of 37 mm, right ventricle of 27 mm, interventricular septum (IVS) of 26 mm, left ventricle of 24 mm, and left atrium of 26 mm. The ejection fraction was 63%, indicating right atrium enlargement, significant thickening of the IVS and left ventricular posterior wall, and a bright band in the left ventricle. False chordae tendineae were considered, and the measured values for left ventricular function were within normal range (*Figure 1C*). Throughout the course of the patient's illness, there is a gradual decline in the functionality of the heart (*Table 1*).

Figure 1 (A) The electrocardiogram (ECG) of the proband. The ECG of the proband revealed left ventricular hypertrophy and ventricular pre-excitation. (B) The ECG of the proband's mother. The ECG of the proband's mother revealed premature ventricular contraction (PVC) and short PR. (C) The magnetic resonance imaging (MRI) of the proband. MRI revealed significant myocardial hypertrophy. Left ventricular short axis, unenhanced (a), enhanced (d); horizontal long axis, unenhanced (b), enhanced (e); left ventricular long axis, unenhanced (c), enhanced (f). (D) The ultrasound colour Doppler of the proband. Ultrasound colour Doppler indicating right atrium enlargement, significant thickening of the interventricular septum (IVS) and left ventricular posterior wall, and a bright band in the left ventricle. IVS thickness was 26 mm. (E) The family tree of Danon disease. Male and female are indicated by squares and circles. The black-filled symbol represents the clinically affected individual. The grey-filled symbol represents the phenotype uncertain individual. The arrow shows the proband.

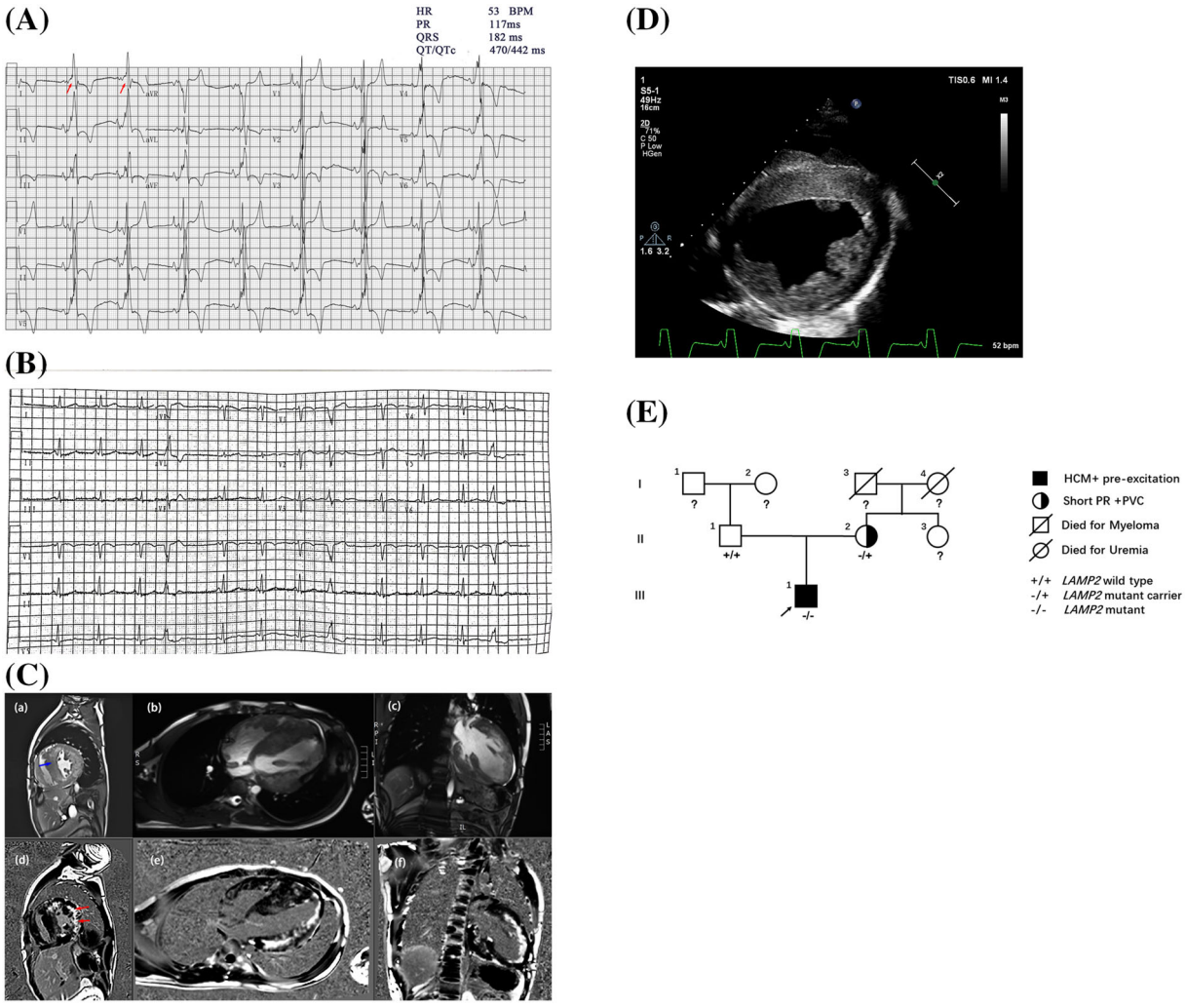

DOI: 10.1002/ehf2.14417

Table 1 Echocardiogram of the patient during follow-up

	18/1/2021	18/2/2021	29/6/2022	20/9/2022	21/3/2023	7/4/2023
LV (mm)	40	50	62	62	68	74
LA (mm)	26	33	31	32	36*40*58	36
RV (mm)	27	29	<42	35	42	42
RA (mm)	37	29	<90	32	42	42
IVS (mm)	26	9	26	22	24	16–24
EF	63%	64%	35%	32%	19%	24%
LVPWd (mm)	24	8	21	16	13	13

EF, ejection fraction; IVS, interventricular septum; LA, left atrium; LV, left ventricle; LVPWd, left ventricular posterior wall in diastole; RA, right atrium; RV, right ventricle.

Cardiac magnetic resonance imaging revealed significant myocardial hypertrophy (*Table 2*). The cardiac cine demonstrated that the left ventricle size was not enlarged; however, the walls of the left ventricle, the free wall of the right ventricle, and the atrial septum displayed uneven thickness, particularly the IVS. Moreover, the left ventricular wall exhibited impaired relaxation and contraction (Supporting Information, *Figure S2*), whereas no obstruction signs were apparent in the left ventricular outflow tract. Myocardial resting perfusion imaging showed numerous patchy perfusion defects in the left ventricular myocardium, as well as beneath the intima of the anterior wall. Similarly, myocardial delayed enhancement imaging (late gadolinium enhancement) exhibited multiple patchy and clustered delayed enhancements in all walls of the left ventricle, with distinct manifestations on the free wall and significant visibility under the intima and within the myocardium (*Figure 1D*).

Initially, we arrived at a diagnosis of hypertrophic cardiomyopathy for the patient and subsequently conducted a comprehensive examination of his family history. In addition, we performed ECG and colour Doppler echocardiography screenings on his family members. Our study revealed that the patient's mother, aged 47, had a short PR interval of 108 ms on the ECG with no symptoms (*Figure 1B*), though her echocardiography results indicated that her cardiac thickness (IVS of 9 mm) was within a normal range. To further verify and elaborate the diagnosis, we strongly recommend that both the patient and his relatives undergo genetic testing.

Table 2 The thickness of left ventricular myocardial segments in magnetic resonance imaging

	Segments		
	Basal	Mid-cavity	Apical
Anterior (mm)	15.4	16.8	12.3
Anteroseptal (mm)	35.1	32.2	14.3[a]
Anterolateral (mm)	22.9	27.1	10.7[b]
Inferior (mm)	23.7	16.9	8.2
Inferoseptal (mm)	23.3	37.4	/
Inferolateral (mm)	29.1	14.7	/

The hypertrophy of the left ventricle is evident, with a thickened interventricular septum.
[a]Septal.
[b]Lateral.

Genetics analysis

After performing filtering and validating through Sanger sequencing, we have identified a pathogenic hemizygous 3′ splice-site mutation, c.864+5G>A, in the intron 6 of the *LAMP2* gene (*Figure 2A*), in accordance with the American College of Medical Genetics and Genomics guidelines. We were unable to locate any additional potential pathogenic variants or SNVs that were associated with hypertrophic cardiomyopathy or ion channelopathy in the coding regions or the flanking regulatory regions. The mutation was also found in his mother (heterozygous) but was not identified in his father (*Figure 2A*).

The gene screening carried out on the patient revealed a replacement mutation in the intron 6 of the *LAMP2* gene, which is predicted to affect gene splicing. This specific mutation is not present in the normal population, and its clinical significance remains unclear. Therefore, based on the patient's clinical manifestation, familial history, and genetic tests, we have diagnosed the patient with a c.864+5G>A mutation in the intron 6 of the *LAMP2* gene, which is associated with Danon disease for the first time.

Splicing study by minigene analysis

We further investigated the impact of the identified 3′ splice-site mutation (c.864+5G>A) in the *LAMP2* gene by minigene assays (*Figure 2C*). The results indicated that the mutation disrupted the splice donor site (GA) within intron 6. We compared the RT-PCR products of both the wild-type and mutant mRNA by electrophoresis, which showed that the mutant cDNA (320 bp) was significantly smaller in size than the wild-type cDNA (443 bp) (*Figure 2B*). By conducting Sanger sequencing, we identified a 123 bp deletion of exon 6 in the mutant cDNA (*Figure 2D*).

Protein structural modelling

The mutant sequence in the cDNA encodes a deletion of exon 6 in the mutant cDNA (*Figure 2D*), resulting in a truncated LAMP2 protein with 369-amino-acid residues. Protein struc-

Figure 2 Clinical and genetic characteristics of the pedigree. (A) Single nucleotide variations and Sanger sequencing of the proband and his parents. (B) DNA electrophoresis of wild-type and mutation gene. MT, mutant type; WT, wild type. (C) The construction of the LAMP2-PET01 minigene plasmid. (D) Sanger sequencing of the plasmid.

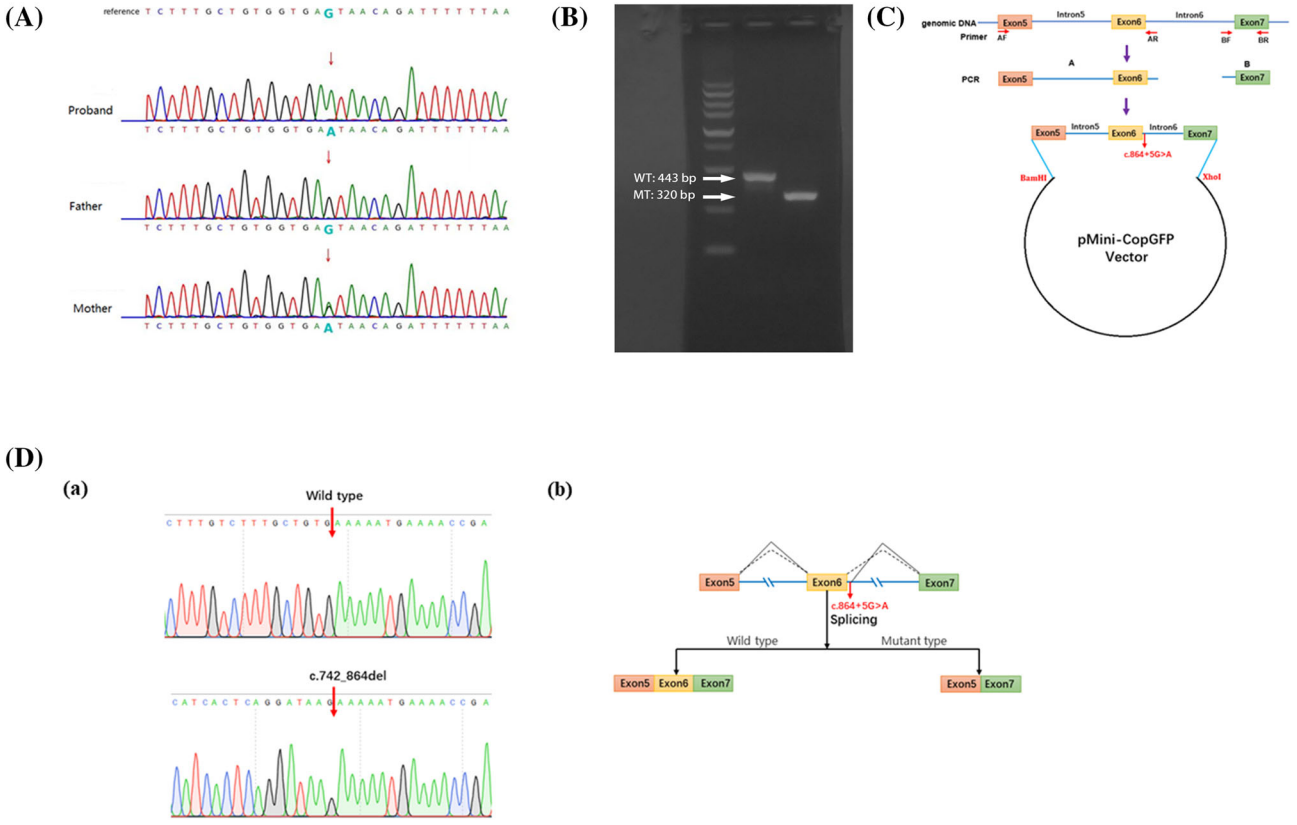

tural modelling results suggest that the mutation causes a protein twists direction change, leading to the conformational change in PyMOL (*Figure 3*).

Discussion

In this study, the proband was diagnosed with Danon disease determined through a combination of clinical examinations, genetic testing, and functional experiments. Using whole-exome sequencing and Sanger sequencing, the heterozygous variant (c.864+5G>A) in the *LAMP2* gene was identified in his mother. Following functional analysis and protein structural modelling, we presented a novel splicing-altering *LAMP2* mutation, resulting in the manifestation of truncated LAMP2 protein and Danon disease syndrome.

Based on the patient's medical history and the results of the ultrasound examination, the initial diagnosis is hypertrophic cardiomyopathy. The possibility of myocardial amyloidosis needs to be ruled out. The clinical manifestations of myocardial amyloidosis include older age, low voltage on ECG, myocardial hypertrophy on echocardiography, but no decrease in ejection fraction. The observation of amyloid deposition on myocardial biopsy is critical for the diagnosis of myocardial amyloidosis.[12] However, in the case of our patient, the early onset age, high ECG voltage, and decrease in ejection fraction suggest that myocardial amyloidosis is unlikely.

Hypertrophic cardiomyopathy is primarily an autosomal dominant inheritance disorder caused by mutations in the gene that encodes the cardiac sarcomere protein. Among the five most frequently occurring genetic variations include myosin binding protein C3 (*MYBPC3*), β-myosin heavy chain (*MYH7*), cardiac troponin T type 2 (*TNNT2*), cardiac troponin I type 3 (*TNNI3*), and α-alpha tropomyosin (*TPM1*).[13] *MYBPC3* mutation is the most common cause of hypertrophic cardiomyopathy. These genetic mutations lead to the production of dysfunctional proteins that are rapidly degraded and fail to integrate into muscle filaments.[14,15] In more than 90% of hypertrophic cardiomyopathy cases related to *MYBPC3* mutations, pre-terminated codons are present and truncated proteins are encoded. Furthermore, *LAMP2* is a metabolic-related gene that affects intracellular glucose metabolism. Positive myocardial biopsy periodic acid-Schiff stain (PAS)

Figure 3 Cartoon model of the LAMP protein structure (residues) by PyMOL. Blue, the wild-type LAMP2 protein; green, the mutant-type LAMP2 protein.

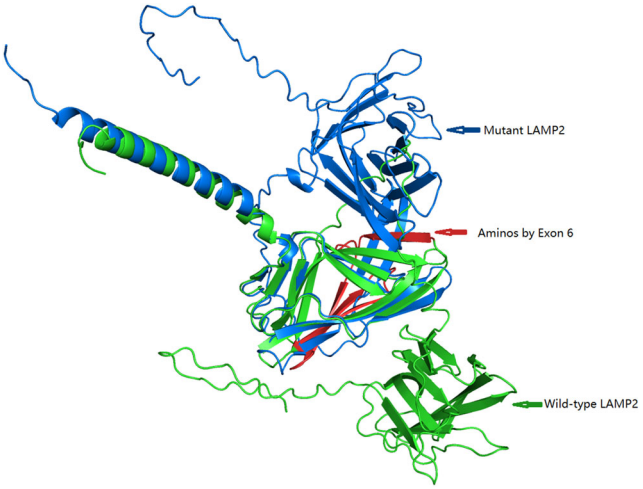

can help identify two types of gene mutations. Thus, we suggested that the patient undergo myocardial biopsy, but the patient and their family refused. Future research could improve myocardial biopsy techniques.

The *LAMP2* mutation was identified in both the proband (hemizygous) and his mother (heterozygous), but it was absent in his father. This suggests co-segregation in the pedigree. Proband's mother carried both a wild-type and a mutant allele and displayed only premature ventricular contraction and short PR interval on ECG without any symptom, consistent with previously reported.[5,16] Minigene assays revealed that the novel splice-site mutation caused the intron 6 splicing in the mRNA (*Figure 2C*). To analyse the function of the new mutant protein, we conducted the AlphaFold2 protein function analysis. In the AlphaFold2 analysis, the mutation truncated the LAMP2 protein to 369-amino-acid residues and caused a protein twist direction change, which resulted in the conformational change (*Figure 3*). Our research findings align with previous studies conducted on Danon disease. Arad *et al*. reported a family with a deletion of *LAMP2* exon 6 that clinically manifested as Danon disease.[17–20] Furthermore, the basic research found that mice with a *LAMP2* gene in-frame deletion of exon 6 developed myocardial hypertrophy in 20 weeks.[21] These findings indicate that exon 6 of the *LAMP2* gene is the key pathogenic gene responsible for Danon disease, which points out guidance for future gene therapy. Our work further illustrates structural differences between the mutant and wild-type LAMP2 proteins (*Figure 3*). Previous research revealed that exon 6 skipping causes loss of two glycosylation sites and abolishes a loop structure by deleting Cys265, which is thought to form a disulfide bond with Cys232, suggesting the importance of exon 6 for LAMP2 function.[2]

The proband exhibits impaired liver function in addition to both myopathy and cardiomyopathy. The pathogenesis of these three organ dysfunctions involves glycogen accumulation in cardiomyocytes, skeletal myocytes, and hepatocytes. The LAMP2 gene mutation leads to lysosomal dysfunction, hindering glycogen digestion and ultimately leading to increased glycogen storage in both the cytoplasm and lysosome. Structural studies utilizing electron microscopy and PAS glycogen staining have provided evidence for glycogen accumulation within cardiomyocytes,[22] skeletal myocytes,[23] and hepatocytes[24] characteristic of Danon disease. Additionally, glycogen accumulation plays a role in cell growth through the Hippo signalling pathway,[25] leading to cardiac hypertrophy, skeletal muscle hypertrophy, and hepatomegaly. Finally, glycogen storage within cells causes cellular damage, evidenced by increased levels of myocardial enzymes, such as cTnT, CK, and CK-MB, and liver enzymes, such as ALT, in the blood (*Figure 4*).

To date, 408 *LAMP2* gene mutant molecular consequences have been reported in the ClinVar database, including 57 frameshifts, 174 missense, 38 nonsense, 28 splice sites, and 111 untranslated regions. The majority of these mutations are pathogenic, with some causing symptoms of Danon disease. Our study reports a new splice-site mutation (c.864 +5G>A) in the *LAMP2* gene. The mutation was not present in the ClinVar database, Exome Aggregation Consortium database, or Human Gene Mutation Database. As mentioned above, 28 splice-site mutations in the *LAMP2* gene are included in the ClinVar database, and 7 of which are located in exon 6 (c.864). These mutations include c.864+3_864+6del,[26] c.864+2T>C, c.864+1del, c.864+1G>A, c.864+1G>T,[5] c.864 +1_864+4del[20,27] (not included in ClinVar), and c.864 +2A>G[20] (not included in ClinVar). Among these, c.864 +1_864+4del,[20] c.864+3_864+6del,[26] c.864+1del, c.864 +1G>T,[5] and c.864+2A>G[20] are predicted to cause altered splicing that leads to an abnormal or absent protein and have been identified as Danon disease-associated mutant gene. The clinical phenotypic spectrum of Danon disease is complex, and

Figure 4 Pathways of glycogen storage in Danon disease. Glucose entry into cells and subsequent conversion into glucose-6-phosphate (G-6-P) facilitated by hexokinase, after which it is targeted for glycolysis or glycogen synthesis by glycogen synthase. Glycogen is stored in the cytoplasm as liver glycogen and muscle glycogen and degraded through the cytoplasmic pathway and lysosomal pathway.

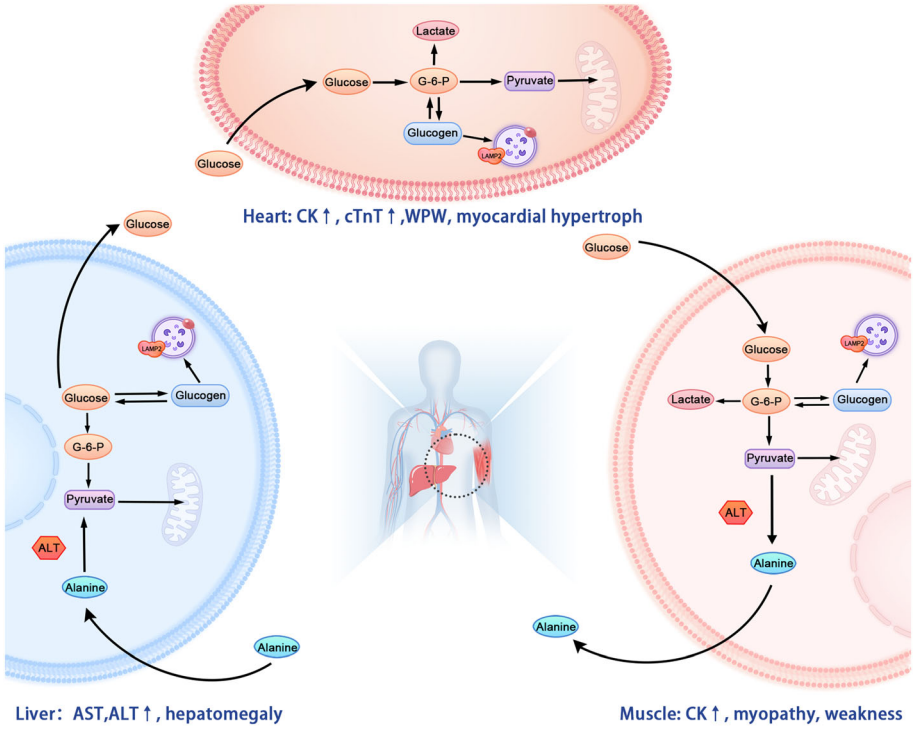

the relationship between different genotypes and clinical phenotypes deserves further exploration.[26]

In conclusion, our study identified a novel splicing-altering variant in the *LAMP2* gene as a pathogenic mutation of Danon disease. Our findings enriched the pathogenic spectrum of the *LAMP2* gene mutation for Danon disease.

Acknowledgements

The authors thank all the referring participants, especially the patient and his family for their participation in this research.

Conflict of interest

The authors confirm that there are no conflicts of interest.

Funding

This work was supported by grants from the National Natural Science Foundation of China (No. 81870336 to D.Q.P.).

Supporting information

Additional supporting information may be found online in the Supporting Information section at the end of the article.

Figure S1. ECGs of the proband from 2021 to 2023. The ECGs show left ventricular hypertrophy and ventricular preexcitation

Figure S2. The LVEF of the proband. The MRI examination reveals a reduction in the LVEF. LVEF, left ventricular ejection fraction; MRI, magnetic resonance imaging.

References

1. Danon MJ, Oh SJ, DiMauro S, Manaligod JR, Eastwood A, Naidu S, Schliselfeld LH. Lysosomal glycogen storage disease with normal acid maltase. *Neurology*. 1981; **31**: 51–57.
2. Nishino I, Fu J, Tanji K, Yamada T, Shimojo S, Koori T, Mora M, Riggs JE, Oh SJ, Koga Y, Sue CM, Yamamoto A, Murakami N, Shanske S, Byrne E, Bonilla E, Nonaka I, DiMauro S, Hirano M. Primary LAMP-2 deficiency causes X-linked vacuolar cardiomyopathy and myopathy (Danon disease). *Nature*. 2000; **406**: 906–910.
3. Dworzak F, Casazza F, Mora M, de Maria R, Gronda E, Baroldi G, Rimoldi M,

Morandi L, Cornelio F. Lysosomal glycogen storage with normal acid maltase: a familial study with successful heart transplant. *Neuromuscul Disord: NMD*. 1994; **4**: 243–247.
4. Zhai Y, Miao J, Peng Y, Wang Y, Dong J, Zhao X. Clinical features of Danon disease and insights gained from LAMP-2 deficiency models. *Trends Cardiovasc Med*. 2021; **33**: 81–89.
5. Boucek D, Jirikowic J, Taylor M. Natural history of Danon disease. *Genet Med*. 2011; **13**: 563–568.
6. Sugie K, Yamamoto A, Murayama K, Oh SJ, Takahashi M, Mora M, Riggs JE, Colomer J, Iturriaga C, Meloni A, Lamperti C, Saitoh S, Byrne E, DiMauro S, Nonaka I, Hirano M, Nishino I. Clinicopathological features of genetically confirmed Danon disease. *Neurology*. 2002; **58**: 1773–1778.
7. D'souza RS, Levandowski C, Slavov D, Graw SL, Allen LA, Adler E, Mestroni L, Taylor MRG. Danon disease: clinical features, evaluation, and management. *Circ Heart Fail*. 2014; **7**: 843–849.
8. Chi C, Riching AS, Song K. Lysosomal abnormalities in cardiovascular disease. *Int J Mol Sci*. 2020; **21**: 10.3390/ijms21030811.
9. Fukuda M. Biogenesis of the lysosomal membrane. *Subcell Biochem*. 1994; **22**: 199–230.
10. Chi C, Leonard A, Knight WE, Beussman KM, Zhao Y, Cao Y, Londono P, Aune E, Trembley MA, Small EM, Jeong MY, Walker LA, Xu H, Sniadecki NJ, Taylor MR, Buttrick PM, Song K. LAMP-2B regulates human cardiomyocyte function by mediating autophagosome-lysosome fusion. *Proc Nat Acad Sci United States Am*. 2019; **116**: 556–565.
11. D'Souza RS, Law L. *Danon Disease*. StatPearls. *StatPearls Publishing Copyright © 2022*. StatPearls Publishing LLC; 2022.
12. Bloom M, Gorevic P. Cardiac amyloidosis. *Ann Intern Med*. 2023; **176**: ITC33–ITC48.
13. Olivotto I, Udelson JE, Pieroni M, Rapezzi C. Genetic causes of heart failure with preserved ejection fraction: emerging pharmacological treatments. *Eur Heart J*. 2023; **44**: 656–667.
14. Pioner J, Vitale G, Steczina S, Langione M, Margara F, Santini L, Giardini F, Lazzeri E, Piroddi N, Scellini B, Palandri C, Schuldt M, Spinelli V, Girolami F, Mazzarotto F, van der Velden J, Cerbai E, Tesi C, Olivotto I, Bueno-Orovio A, Sacconi L, Coppini R, Ferrantini C, Regnier M, Poggesi C. Slower calcium handling balances faster cross-bridge cycling in human *MYBPC3* HCM. *Circ Res*. 2023; **132**: 628–644.
15. Marian A, Braunwald EJC. Hypertrophic cardiomyopathy: genetics, pathogenesis, clinical manifestations, diagnosis, and therapy. *Circ Res*. 2017; **121**: 749–770.
16. Cenacchi G, Papa V, Pegoraro V, Marozzo R, Fanin M, Angelini C. Review: Danon disease: review of natural history and recent advances. *Neuropathol Appl Neurobiol*. 2020; **46**: 303–322.
17. Cheng Z, Cui Q, Tian Z, Xie H, Chen L, Fang L, Zhu K, Fang Q. Danon disease as a cause of concentric left ventricular hypertrophy in patients who underwent endomyocardial biopsy. *Eur Heart J*. 2012; **33**: 649–656.
18. Luo SS, Xi JY, Cai S, Zhao CB, Lu JH, Zhu WH, Lin J, Qiao K, Wang Y, Ye ZR. Novel LAMP2 mutations in Chinese patients with Danon disease cause varying degrees of clinical severity. *Clin Neuropathol*. 2014; **33**: 284–291.
19. Sugie K, Yoshizawa H, Onoue K, Nakanishi Y, Eura N, Ogawa M, Nakano T, Sakaguchi Y, Hayashi YK, Kishimoto T, Shima M, Saito Y, Nishino I, Ueno S. Early onset of cardiomyopathy and intellectual disability in a girl with Danon disease associated with a de novo novel mutation of the LAMP2 gene. *Neuropathology*. 2016; **36**: 561–565.
20. Arad M, Maron BJ, Gorham JM, Johnson WH Jr, Saul JP, Perez-Atayde AR, Spirito P, Wright GB, Kanter RJ, Seidman CE, Seidman JG. Glycogen storage diseases presenting as hypertrophic cardiomyopathy. *N Engl J Med*. 2005; **352**: 362–372.
21. Alcalai R, Arad M, Wakimoto H, Yadin D, Gorham J, Wang L, Burns E, Maron BJ, Roberts WC, Konno T, Conner DA, Perez-Atayde AR, Seidman JG, Seidman CE. LAMP2 cardiomyopathy: consequences of impaired autophagy in the heart. *J Am Heart Assoc*. 2021; **10**: e018829.
22. Piotrowska-Kownacka D, Kownacki L, Kuch M, Walczak E, Kosieradzka A, Fidzianska A, Krolicki L. Cardiovascular magnetic resonance findings in a case of Danon disease. *J Cardiovasc Magn Reson*. 2009; **11**: 12.
23. Papa V, Tarantino L, Preda P, Badiali de Giorgi L, Fanin M, Pegoraro E, Angelini C, Cenacchi G. The role of ultrastructural examination in storage diseases. *Ultrastruct Pathol*. 2010; **34**: 243–251.
24. Furuta A, Wakabayashi K, Haratake J, Kikuchi H, Kabuta T, Mori F, Tokonami F, Katsumi Y, Tanioka F, Uchiyama Y, Nishino I, Wada K. Lysosomal storage and advanced senescence in the brain of LAMP-2-deficient Danon disease. *Acta Neuropathol*. 2013; **125**: 459–461.
25. Liu Q, Li J, Zhang W, Xiao C, Zhang S, Nian C, Li J, Su D, Chen L, Zhao Q, Shao H, Zhao H, Chen Q, Li Y, Geng J, Hong L, Lin S, Wu Q, Deng X, Ke R, Ding J, Johnson RL, Liu X, Chen L, Zhou D. Glycogen accumulation and phase separation drives liver tumor initiation. *Cell*. 2021; **184**: 5559–5576.e19.
26. Bui YK, Renella P, Martinez-Agosto JA, Verity A, Madikians A, Alejos JC. Danon disease with typical early-onset cardiomyopathy in a male: focus on a novel LAMP-2 mutation. *Pediatr Transplant*. 2008; **12**: 246–250.
27. Yoshida S, Nakanishi C, Okada H, Mori M, Yokawa J, Yoshimuta T, Ohta K, Konno T, Fujino N, Kawashiri MA, Yachie A, Yamagishi M, Hayashi K. Characteristics of induced pluripotent stem cells from clinically divergent female monozygotic twins with Danon disease. *J Mol Cell Cardiol*. 2018; **114**: 234–242.